

Geometrically Thin Disk Accreting Into a Black Hole

N. A. Shorod & B. Paczynski

Princeton University Observatory, Princeton, NJ 08544 (1001, USA)

E-mail: ashorod@astro.princeton.edu

E-mail: bp@astro.princeton.edu

ABSTRACT

A numerical model of a steady state, thin accretion disk with a constant effective speed of sound is presented. We demonstrate that 'zero torque' inner boundary condition is a reasonable approximation provided that the disk thickness, including the thickness of the torquing magnetic fields, is small. It is likely that this conclusion is correct also for non-steady disks, as long as the total thickness at the inner edge, H_{in} , is much smaller than the radius there, $r_{in} \ll r_{in}$. The very existence of thin disks is not proved or disproved in this work, but such disks are believed to exist for moderate accretion rates. An important result of our analysis is that the physically acceptable steady state solutions in our toy model exist only for $v_s < 0.14 (100v_s = c)^{1/3}$.

A significant torque may be applied to a thin disk if there is a large scale magnetic field, like in a modified Blandford-Znajek mechanism.

Subject headings: black hole physics | accretion disks | magnetic fields

1. Introduction

A Newtonian theory of geometrically thin accretion disks was developed in classical papers by Pringle & Rees (1972), Shakura & Sunyaev (1973) and Lynden-Bell & Pringle (1974), generalized for a relativistic case by Novikov & Thorne (1973), and reviewed by Pringle (1981). A relativistic effect: the bending of light trajectories leading to direct illumination of the disk by itself, was first elaborated and calculated by Cunningham (1975, 1976). This is marginally important for a disk accreting onto a Schwarzschild black hole, but it is important in the Kerr case, introducing significant non-local effects to the energy balance at small radii. In these early papers a geometrically thin disk accreting onto a black hole had the inner boundary at the marginally stable orbit, r_{in} , and the gas was freely falling on a tight spiral inwards of r_{in} .

There was some confusion about the nature of gas flow near the inner disk edge (Stoeger 1976). The issue was first understood as a transition from sub-sonic accretion to supersonic accretion for geometrically thick disks (Abramowicz et al. 1978), and later for geometrically thin disks (Machotrzew & Paczynski 1982). Small parameter used in these papers resulted in saddle-type critical points. Matsumoto et al. (1984) found that for moderately large values of the critical point was nodal-type. These papers, and many more, were reviewed by Abramowicz & Kato (1989), who presented a general discussion of the transonic flows in accretion disks. In particular, they pointed out that while such a transition is necessary for the existence of a steady state accretion, it does not guarantee that a sensible global solution exists (cf. their Fig. 2).

All the papers written in 1970s and 1980s adopted some form of 'alpha' viscosity, as there was no quantitative physical model for the effective transport of angular momentum and the dissipation of energy within accretion disks. Perhaps the best qualitative description of these processes was given by Galyev et al. (1979). A major breakthrough was made by Balbus & Hawley (1991) and Hawley & Balbus (1991), who rediscovered a powerful magneto-rotational instability in weakly magnetized disks, and pointed out its relevance to accretion. A host of papers followed, with powerful computers making it possible to model time dependent accretion flows in 2-D (Armitage 1998, Stone et al. 1999, Agol et al. 2001, Stone & Pringle 2001, and references therein) and in 3-D (Flemming et al. 2000, Hawley et al. 2001, Armitage 2001a,b, Armitage et al. 2001, Reynolds & Armitage 2001, Reynolds et al. 2001, Sano & Inutsuka 2001, Krolik & Hawley 2002, Hawley & Krolik 2002, and references therein).

A lot of semi-analytical and numerical work was done for the ADAF and CDAF models (cf. Bal, Narayan & Quataert 2001, and references therein). It appears that at very high and at very low accretion rates disks are geometrically thick, while thin disks may exist only for moderate accretion rates. If this view is correct then the early work on geometrically thin accretion disks may be relevant for $0.01 < L = L_{Edd} < 0.1$.

Yet another way to modify the picture was proposed by Blandford and Znajek (1977), who pointed out that a large scale magnetic field may thread a black hole, and it may extract its rotational energy. In recent years the original picture was modified, making it more likely that the energy extracted from a spinning black hole is transferred to the inner parts of the disk, rather than directly to a distant load (Agol & Krolik 2000, Li 2000a,b, Wang et al. 2002, and references therein). Recent XMM observations of an AGN named MCG -6-30-15 were claimed to support this possibility (Wills et al. 2001).

In addition to the diversity of disk models a traditional concept of no torque inner boundary condition was challenged by Krolik (1999), Gammie (1999), and Agol & Krolik

(2000) even for geometrically thin disks with steady state accretion. One of us (BP) could not agree with their claim, and presented simple arguments why a no torque inner boundary condition is natural if an accretion disk is geometrically thin (Paczynski 2000), but the referee could not be convinced. Thanks to the electronic preprint server this paper is readily accessible to all interested readers, who can judge its validity.

While the author (naturally) is convinced that he was right, he did not fail to notice that his arguments while simple were not convincing. Apparently, the arguments were not clear enough, and they were not complete. As far as we can tell the main reason for the controversy was the imprecise and ambiguous term *inology* used by Paczynski (2000). The purpose of this paper is to outline the simple reasoning behind thin disk models of 1970s and 1980s, to present the arguments for the no torque inner boundary condition, the assumptions involved, and to present a simple model as an example. We are doing our best to clarify our terminology.

In Sec. 2, we derive the equations that describe a thin and steady state accretion disk with a fixed value of the effective speed of sound, while in Sec. 3, solutions of these equations and their topologies are studied numerically. Sec. 4, describes an analytical method to identify solutions of different nature. In Sec. 5 we discuss some of the physical results of our work as well as those of Gammie (1999), and finally, Sec. 6 concludes this paper.

2. A Thin Disk

The modern 2-D and 3-D numerical simulations provided the first quantitative and meaningful insight into the actual physics of angular momentum transport in accretion disks. As computer power increases and the codes become more sophisticated a steady progress is to be expected. However, at this time there are significant limitations. The accretion flows are relatively thick, the outer boundary is not very far out, the cooling processes are not included, the time integrations can be carried out for a rather modest multiple of the dynamical time scale. Hence, when it comes to modelling disk spectra, conventional steady state, geometrically thin disk models are still commonly used (e.g. Blaes et al. 2001). The current ADAF or CDAF or variants of Blandford - Znajek models do not exceed a toy model level. This is both, natural and useful, and the quantitative understanding will be improved with time. For the same reason it is useful to have a good quantitative understanding of semi-analytical models of geometrically thin accretion disks. The simple toy models will remain useful even when the 3-D numerical approach provides full quantitative comparison with the future observations.

The argument presented by Paczynski (2000) in favor of applicability of a no torque inner boundary condition was very simple. Geometrically thin, steady state disk accretion onto a black hole was sub-sonic at $r > r_{in}$, and supersonic at $r < r_{in}$, with the inner disk radius r_{in} located near the marginally stable orbit, at r_{ms} . The specific angular momentum at r_{in} is l_{in} , and it satisfies the equation

$$\frac{l_{in}}{l_0} \leq \frac{H_{in}}{r_{in}} \leq 1; \quad \text{if} \quad 1 \quad \text{and} \quad \frac{H_{in}}{r_{in}} \leq 1 \quad (1)$$

(cf. eq. 4 in Paczynski 2000), where l_0 is the angular momentum integration constant, H is the disk thickness, and η is the viscosity parameter. The eq. (1) follows from angular momentum conservation in a steady state accretion flow. Current 3-D numerical calculations for thick disks and tori indicate $\eta \approx 0.1$, with large fluctuations of all physical quantities. The inequality (1) is equivalent to the no torque inner boundary condition, or more precisely to a very small torque at the inner disk edge. This conclusion remains valid even for $\eta = 1$, as long as $H_{in} = r_{in} \ll 1$, i.e. as long as the disk remains geometrically thin at the critical point. Note, the eq. (1) is local, i.e. it does not matter if the parameter η is constant throughout the flow, or does it vary with radius. The two essential assumptions are that the disk is geometrically thin, and that the accretion is steady state.

What can be wrong with eq. (1)? There are several possibilities. Thin disks, with $H_{in} = r_{in} \ll 1$ may be physically impossible. We do not know if this is true or not, as we have neither theoretical nor observational proof either way. Steady state accretion may not exist in nature. Current 3-D simulations have indicated that strict steady state flow is not possible, but there is a possibility that when averaged over moderate time scale a quasi steady state may still be a sensible approximation. The eq. (1) may hold as long as the fluctuating disk thickness remains small at all time. This domain is not accessible to numerical calculations so far. Next, there is a global problem pointed out by Abramowicz & Kato (1989): an accretion flow may pass through a sonic point near r_{ms} but it may not continue all the way into a black hole, as shown schematically in their Fig. 2. In fact, we could not find any reference from 1980s demonstrating that the supersonic infall for $r < r_{ms}$ continues all the way. This was assumed to be obvious and the global flow pattern was not verified numerically.

Finally, there is an issue of terminology: what does it mean that a disk is geometrically thin? In the eq. (1) the disk thickness H refers to the structure which carries stresses. If the stresses which make the accretion possible are magnetic, as seems to be very likely, then H must refer to the geometrical thickness of the magnetic field structure, not just the gas layer. The notion that the magnetic thickness may be larger than gas thickness dates back at least to Galyeyev et al. (1979), and has found some support in recent 2-D and 3-D simulations. Even more importantly, all Bondi-Znajek type models are based on large

scale magnetic structures to transfer momentum and energy. The distinction between the magnetic and gas disk thickness was not considered at all in the classical papers about disk accretion, and it was not mentioned by Paczynski (2000). Yet, it is the scale height of the stresses that is important for eq. (1). Therefore, we emphasize that the term : 'geom etrically thin disk' refers to the thickness of magnetic structures responsible for the momentum transfer.

Another source of ambiguity comes with the term 'pressure' and . There are many different ways in which the parameter has been defined in the literature. In the original work of Shakura & Sunyaev (1973), was defined as the ratio of tangential stress to the pressure of the the viscous uid. Balbus & Hawley (1991), recognized that this stress is in fact dominated by the magnetic terms. Early simulations seemed to indicate that the gas pressure dominates the magnetic pressure, at least outside the marginally stable orbit. Recent 3-D simulations (e.g. Hawley & Krolik 2002) show that magnetic pressure may dominate the gas pressure inside the marginally stable orbit. Therefore, we define in terms of total pressure, including magnetic, so it cannot exceed 1. It is not essential for our model to have constant value of , this is just the simplest assumption.

Another ambiguity is caused by the 'speed of sound'. It is conventionally defined as the speed at which gas pressure disturbances propagate, or it may also include the effects of radiation pressure. If the magnetic pressure dominates then the Alfvén speed becomes much larger than the speed of sound. Rather than study the complicated effects of different speeds at which different disturbances may propagate we introduce the 'effective speed of sound' $v_s = (P =)^{1/2}$, where P is the total pressure, which is relevant for the v_s . With highly tangled magnetic fields this seems to be a reasonable, though perhaps non-orthodox definition. It is the effective speed of sound (the fast magnetosonic speed) that defines the transition from a sub-sonic to a supersonic flow. It is beyond the scope of this paper to provide a rigorous justification of our approach, but we think this simplification is sensible. For a disk to remain geom etrically thin it is essential that the effective speed of sound is much smaller than the speed of light, but it does not have to be constant. A theory which would allow us to calculate the effective speed of sound from the first principles does not exist. Therefore, we consider the simplest possible disk model, and we assume that throughout the disk the 'effective speed of sound' remains constant, ie. $v_s = \text{const}$. This assumption is not essential, it is just the simplest.

We should note that a key ingredient in the above arguments, and in the analysis of the following sections, is the assumption of hydrostatic equilibrium in the direction perpendicular to the disk. The reason for this assumption is that, for a thin disk, the dynamical time associated with the vertical direction is a fraction of the rotational period

which remains much less than the infall time until far down into the supersonic regime, where the infall speed is comparable to the speed of light. The result of this assumption is that the effective speed of sound is always much less than the Keplerian velocity, as long as the disk remains thin (cf. eq.(5a)).

Following all these definitions we present a simple thin accretion disk model in order to demonstrate that there is no problem of the type envisioned by Abramowicz & Kato (1989), i.e. that once the infall becomes supersonic it never 'turns back'. Our simple numerical model reproduces the basic features of classical thin disks, and demonstrates that the transonic solution may remain unique not only for a saddle, but also for a nodal critical point. But first we recall some concepts of the thin disk models of several decades ago. For the derivation of all equations the reader may consult the paper by Abramowicz & Kato (1989).

The single most important difference between Newtonian accretion and an accretion onto a black hole is the presence of a marginally stable orbit in the latter. Newtonian gravity varies strictly as a power of radius, therefore binding energy and the Keplerian angular momentum vary as power laws of radius, and this makes self-similarity an acceptable simplifying assumption for some accretion flows. This is not the case in general relativity: at small radii 'Keplerian' quantities are no longer power laws of radius, they do not even vary monotonically. The 'Keplerian' angular momentum and the corresponding binding energy reach a minimum at r_{ms} , the radius of a marginally stable orbit. This feature can be reproduced with a pseudo-Newtonian potential (Paczynski & Wita 1980):

$$= \frac{GM}{r - r_g}; \quad r_g = \frac{2GM}{c^2}; \quad (2)$$

For a test particle on a 'Keplerian' circular orbit we have a relation

$$\frac{d}{dr} = \frac{GM}{(r - r_g)^2} = \frac{v_K^2}{r}; \quad (3)$$

where v_K is the 'Keplerian' rotational velocity. It follows that 'Keplerian' angular momentum, l_K , angular velocity, ω_K , and binding energy, e_K , are given as

$$l_K = v_K r = (GM r)^{1/2} \frac{r}{r - r_g}; \quad \omega_K = \frac{v_K}{r} = \frac{GM}{r^3} \frac{1}{r - r_g}; \quad (4a)$$

$$e_K = + \frac{v_K^2}{2} = \frac{GM (r - 2r_g)}{2 (r - r_g)^2} \quad (4b)$$

At very large radii, $r=r_g \rightarrow 1$, the eqs. (2-4) asymptotically become Newtonian, but the differences are large at small radii. In particular, a minimum value of 'Keplerian' angular

momentum and binding energy is reached at $r = r_{\text{ms}} = 3r_g$, just as it does in the relativistic Schwarzschild case. The orbits with $r > r_{\text{ms}}$ are stable, while those with $r < r_{\text{ms}}$ are unstable, with a marginal stability at r_{ms} .

Let us consider the simplest disk model with zero pressure. In this case all stream lines are identical with particle trajectories, i.e. they are nested 'Keplerian' orbits. This structure can be extended to small radii, but all orbits inwards of r_{ms} are unstable: a small perturbation makes a particle spiral into a black hole. Therefore, a zero pressure disk is truncated at r_{ms} , it cannot extend inwards of r_{ms} . Such a disk has zero geometrical thickness, and it is static, i.e. there is no accretion.

To make disk accretion possible it is necessary to introduce some means of angular momentum exchange between nearby stream lines. In general, this will require a non-zero total pressure P , a non-zero effective speed of sound v_s ($P = \frac{1}{2}v_s^2$), and a finite disk thickness H . For simplicity we assume the effective speed of sound to be constant:

$$\frac{H}{r} = \frac{v_s}{v_K} = 1; \quad v_s = \text{const}; \quad \frac{v_s^2}{c^2} = \frac{P}{c^2} = 1; \quad = dz; \quad (5a)$$

We remind the reader that pressure P is the total pressure:

$$P_{\text{tot}} = P_{\text{gas}} + P_{\text{rad}} + P_{\text{mag}} + P_{\text{turb}}; \quad (5b)$$

The effective speed of sound v_s becomes close to Alfvén speed when the magnetic pressure dominates.

We assume that the stresses responsible for angular momentum transport are proportional to the total pressure and the shear rate. The torque exerted by these stresses across radius r is

$$g = 2 r^2 \frac{1}{K} \frac{d}{d \ln r} \int_0^z P dz = 2 r^2 \frac{d \ln}{d \ln r} \frac{1}{K} v_s^2; \quad (6)$$

The dimensionless factor is assumed to be less than unity, and for simplicity we take it to be constant. Again, just as it was the case with the 'effective speed of sound', the assumption that is constant is not essential, it is just the simplest. Note, that varies monotonically with radius, i.e. the inner disk rotates faster, and angular momentum is transported outwards.

The P term, no matter how small, redistributes angular momentum within the disk, and accretion becomes possible. In a steady state each disk element gradually loses its angular momentum, and slowly spirals inwards. For $r > r_{\text{ms}}$ the process can be envisioned as a motion along ever smaller nearly 'Keplerian' orbits, with gradually decreasing angular

momentum. This brings matter close to r_{m_s} . Following any additional loss of angular momentum the gas cannot find any Keplerian' orbit and must plunge into the black hole along a spiral, approximately conserving angular momentum.

Let us assume a steady state, with the mass accretion rate $\dot{M} = \text{const} < 0$, and the radial flow velocity $v_r < 0$ assumed to be a function of radius only. The conservation laws of mass and angular momentum are

$$\dot{M} = 2 \pi r v_r; \quad g = \dot{M} (1 - \frac{1}{r}); \quad (7)$$

where \dot{M} is the integration constant (cf. Abramowicz & Kato 1989). Combining eqs. (6) and (7) we obtain

$$(\gamma) (1 - \frac{1}{r}) = r v_s^2 \frac{d \ln \frac{1}{r}}{d \ln r} \frac{!}{K} : \quad (8)$$

It is reasonable to expect that $\dot{M} = \dot{M}_s$ (to be verified later), and the last equation may be used to estimate the radial flow velocity in the nearly Keplerian' thin disk for $r > r_{m_s}$ and $\gamma_r \neq v_s \neq 1$.

Note, that in eq. (8) only two quantities vary a lot within the flow: v_r and $(1 - \frac{1}{r})$, while the others are either constant or vary slowly. In particular, according to the classical theory of thin accretion disks, near the r_{m_s} and inwards of r_{m_s} angular momentum is almost conserved. This implies that

$$\frac{d \ln \frac{1}{r}}{d \ln r} = 2; \quad \text{therefore} \quad (\gamma) (1 - \frac{1}{r}) = 2 r v_s^2 \frac{!}{K} : \quad (9)$$

The numerical solutions of the following sections will verify this assumption.

We expect that when matter reaches $r = r_{m_s}$ any additional loss of angular momentum puts it on a spiral infall toward the black hole, during which energy and angular momentum are approximately conserved, i.e.

$$e = \frac{GM}{r} + \frac{v_r^2}{2} + \frac{v_{\text{rot}}^2}{2} \quad \dot{E}_s = \frac{c^2}{16}; \quad l = v_{\text{rot}} r \quad \dot{l}_s = 3^{1/2} \frac{GM}{c}; \quad (10)$$

where v_{rot} is the rotational velocity component of the infall. This is verified with the numerical integrations in the following sections.

To calculate a transition from the sub-sonic radial flow to the supersonic flow we need the equation of motion (cf. Abramowicz & Kato 1989)

$$v_r \frac{dv_r}{dr} + \frac{v_r^2}{r} + \frac{v_s^2}{r} + \frac{v_s^2}{2} \frac{d \ln \frac{1}{r}}{dr} = 0: \quad (11)$$

{ 9 }

Differentiating the mass conservation law (eq. 7) we obtain

$$\frac{v_s^2}{r} \frac{d}{dr} = \frac{v_s^2}{r} - \frac{2}{r^2} + \frac{d \ln v_r}{dr}; \quad (12)$$

and combining eqs. (11) and (12) we find

$$v_r^2 - \frac{2}{r^2} + \frac{d \ln v_r}{d \ln r} - \frac{1}{r^2} + \frac{d \ln \frac{v_r}{r}}{d \ln r} - 1 = 0; \quad (13)$$

We introduce dimensionless constants and variables defined as

$$a = \frac{v_s}{c} = 1; \quad b = \frac{1}{\ln s} = 1; \quad 0 < < 1; \quad (14a)$$

$$! = \frac{v_r}{c}; \quad v = \frac{v_r}{c} > 0; \quad x = \frac{r}{r_g}; \quad (14b)$$

The equation of motion (13) and conservation of angular momentum (9) may be written in dimensionless form as

$$\frac{d \ln v}{d \ln x} = \frac{1}{(v^2 - a^2)} - \frac{1}{2(x-1)^2} + 2.5 a^2 \frac{x^{0.6}}{x-1}; \quad (14)$$

$$! = \frac{1.5}{x} \frac{b(x-1)v}{x^{1.2} v^2 - \frac{p}{2} \frac{b}{2} a^2 (x-1)}; \quad (15)$$

3. Critical Points, Physical Solutions and their Topology

We seek a physical solution which has the properties

$$v=a = 1; \quad ! = 1; \quad \text{for } x = 3; \quad (16a)$$

$$v = a; \quad \text{for } x = x_c; \quad (16b)$$

$$v=a = 1; \quad \text{for } x = x_c; \quad (16c)$$

i.e. the flow is sub-sonic and the disk is 'Keplerian' at large radii, the flow passes through a critical point, and it becomes supersonic at small radii.

To better understand the behavior of the physical solutions of eq. (14), and to be able to integrate it numerically near the critical point, we decompose it into two equations

$$\frac{d \ln v}{dt} = \frac{1}{2(x-1)^2} + 2.5 a^2 \frac{x^{0.6}}{x-1}; \quad (17a)$$

$$\frac{d \ln x}{dt} = v^2 - \alpha; \quad (17b)$$

which, together with eq. (15), form a two-dimensional autonomous dynamical system. The variable t , is a dummy variable and should not be confused with physical time.

As mentioned earlier, the physical solution must pass a critical point to reach the supersonic regime, otherwise the solution would not be single-valued as the right hand side of eq. (14) diverges. Now, the critical points of eq. (14) are the fixed points of eqs. (17) and an understanding of the nature of these fixed points is necessary for constructing a physical solution.

At any fixed point, the right hand sides of eqs. (17) vanish. Eq. (17b) implies that fixed points are always at $v = a$, as required by eq. (16b). The right hand side of eq. (17a) at the critical point, together with eq. (15) (with $v = a$) lead to a complicated algebraic equation for x at a given b , or vice versa. The analysis is significantly simplified for small values of a and the corresponding relation between b and x_c is shown in Fig. 1. We see that, in general, there are either no fixed points or two fixed points in the system, while at the critical value of $b = 1 + O(a)$, there is only a single degenerate fixed point at $x = 3$.

The nature of the fixed points can be investigated analytically by linearizing eqs. (17) around each of them. It turns out that the left fixed point (smaller value of x) is always saddle-like, i.e. the two eigenvalues have opposite signs. The right fixed point is of the spiral type (two complex eigenvalues) when the two fixed points are far apart, but it switches to the nodal type (two eigenvalues of the same sign) as the two fixed points get closer. This behavior is shown in Figs. 2-5 which is the typical behavior of a saddle-node bifurcation (Guckenheimer & Holmes 1983).

The integrations presented in Figs. 2-5 were calculated numerically, except near the critical points, where an analytic expansion was used. All four figures have the same disk parameters: $a = v_s = c = 0.01$ and $\alpha = 0.15$. They differ in the adopted value of the angular momentum constant b . The family of solid lines shown in each figure represents possible solutions of the eq. (14). The solutions of special interest for us are those which satisfy boundary conditions (16a,b,c). As it turns out none of these figures has a desired solution, but the figures present the changes in the structure of the critical points.

Fig. 2 presents a saddle critical point at $x_c = 2.7$, and a spiral point at $x_c = 3.4$. The Phase Portraits for $b > 0.9997$ (including $b > 1$) is qualitatively similar to Fig. 2. The Phase Portrait changes when the angular momentum constant b is reduced, as shown in Fig. 3, where the two critical points are saddle at $x_c = 2.94$, and nodal at $x_c = 3.1$. When b is reduced down to $b = 0.9947$ the two critical points merge, as shown in Fig. 4. This corresponds to the point marked $(x_c; 1)$ in Fig. 1. When b is reduced even more then there

is no critical point, as demonstrated with Fig. 5, and as was anticipated (cf. Fig. 1).

A prominent feature of Figs. 2-5 is the Keplerian' solution. In the sub-sonic regime, (v \approx a), the the right hand side of eq. (14) is very large for small values of a unless $\beta \approx 1$ (almost Keplerian' angular velocity). This implies that the only slowly varying solution of eq. (14) is an almost Keplerian' one. The radial velocity for a Keplerian' solution is obtained by setting $\beta = 1$ in eq. (15),

$$v_0 = \frac{2^{\frac{p}{2}} a^2 x}{x^{\frac{3-p}{2}} (x-1)^{\frac{p}{2}} 1.5^{\frac{3-p}{2}} b} + O(a^4); \quad (18)$$

Figs. 2-5 show that all the other solutions tend to merge with the Keplerian' solution as x decreases. This implies that the behavior of the physical solution close to r_m is almost independent of the boundary condition at large radii, since all different solutions merge as they move inwards. Therefore, it is easy to satisfy the boundary condition given with eq. (16a). However, none of the solutions shown in Figs. 2-5 satisfies all three conditions given by eqs. (16a,b,c).

It is clear that a physical solution may pass through a saddle or a nodal xed point, but not a spiral. Furthermore, we assume that a physical solution is analytic. This singles out only two ways of passing a nodal xed point (slow or fast modes), because a linear superposition of fast and slow modes is non-analytic (when v is expressed as a function of x). In the case of a saddle xed point, only two solutions (in the direction of two eigenvectors) can pass the xed point. A conclusion that can be drawn from this consideration is that, in general, the Keplerian' solution does not analytically pass the xed points and only for discrete values of the angular momentum constant b a physical solution is possible.

Now, we are ready to analyze different topologies that can occur in the parameter space of our model. For a given value of a the nature of critical points can be calculated analytically for any pair of values of β and x_c , or equivalently β and b . Fig. 6 shows the possibilities for $a = v_s = c = 0.01$. The horizontal axis, x , is the position of a xed point and the vertical axis is the parameter β that appears in the viscosity model (eq. 5). The xed points are of the saddle-type, on the left side of the dashed region, of the nodal-type inside the dashed region, and of the spiral-type on the right side of the dashed region. The solid curve aB C d shows the position of physical solutions that allow passage of the Keplerian' curve through the critical point. The critical points present in Figs. 2-4 are indicated in Fig. 6 with diamonds numbered 2, 3, 4, 3, and 2, correspondingly, with $\beta = 0.15$ for all of them. The diamonds with numbers 7, 9, and 11, correspond to critical points presented in Figs. 7, 9, 11; they are all located on the solid line aB C d.

We note that for smaller than some critical value β_{SN} , the physical critical point is

of the saddle type (segment aB), while for larger values of α it is of the nodal type (segment Bd). The value of s_N depends on α . For example for $\alpha = 0.01$ we have $s_N = 0.08$ (cf. Fig. 6).

A critical point of the saddle type, shown in Figs. 7 and 8, is the type that is usually encountered in astrophysics. The best known examples are the solar wind (Parker 1958) and Roche lobe overflow in binary stars. As argued above, when the parameters α and β are fixed then physical solution exists only for a unique value of b and the corresponding value of x_c .

In the case of a nodal critical point, the passage is possible through fast or slow¹ directions. However, a generic solution, which is a combination of fast and slow modes, passes the critical point in the slow direction since the slow solution dominates the fast one close to the critical point. In this sense, a physical solution that passes a nodal point in the fast direction, is unique, similar to the saddle critical point. This kind of passage is seen in the BC section of the aB C d curve in Fig. 6 and an example of the phase portrait is shown in Figs. 9 and 10. Note that, again similar to the saddle point solutions, there is a smooth transition from the sub-sonic to the supersonic regime.

Finally, the physical solution may pass the critical point in the slow direction. However, as argued above, this does not fix the value of b since it is the generic behavior of the solutions, and only by requiring the analyticity of the physical solution one may determine b uniquely. The points on the C d segment in Fig. 6 are of this type, and an example of the phase portraits is plotted in Figs. 11 and 12.

The transition from the former type of nodal passage to the latter occurs at α_N . For example, for $\alpha = 0.01$, $\alpha_N \approx 0.14$ (point C in Fig. 6). The curve aB C d, at the transition point C, is tangent to the boundary of the nodal and saddle regions, where the fast and slow directions merge.

The main difference between the last type of passage and the previous two types is that there is a sharp change in slope, right after passing the critical point. The reason is that the Keplerian' curve, which is connected to the slow direction, turns from stable (as x decreases) in the sub-sonic regime to unstable in the supersonic regime, and so the physical solution departs from the Keplerian' curve after the passage. Since the slopes are significantly larger far from the Keplerian' curve, there is a sharp change in slope.

While we have described some properties of solutions with a nodal critical point, a general discussion of these matters is beyond the scope of this paper. The central issue

¹The fast/slow direction refers to the direction of the eigenvector with the larger/smaller eigenvalue.

for us is the inner boundary condition for a steady state geometrically thin accretion disk. For a given value of the effective speed of sound $v_s = ac$, and for $a = 0.14$ we found a unique numerical solution, in agreement with the finding of Abramova et al. (2001). We verified the uniqueness of numerical solution in two ways. First, we began with a guess of the location of the critical point x_c , and we searched for the value which provided a solution close to 'Keplerian' at large radii. This provided a unique value of the angular momentum constant b for the given a and v_s . We also started numerical integrations of the eqs. (17 and 15) at large radii, where we adopted a 'Keplerian' model. We searched for the value of the angular momentum constant b for which the solution would pass through the critical point. There was a unique value of b and x_c found for the given a and v_s and it was identical to that found with the first method. There was no difference in the numerical procedure for solutions which had a saddle or a nodal critical point.

We found that for $a = 0.01$ and $0.01 < a < 0.14$ there are unique solutions for the sub-sonic, steady state flow with the effective speed of sound assumed to be constant. The critical point location varied monotonically in the range $2.8286 < x_c < 3.1058$ and the angular momentum constant varied monotonically in the range $1.00068 < b < 0.99528$, i.e. we had $x_c = x_{s1} = 3.0$ and $b = 1.0$. These results are not in any way affected by the supersonic flow at $x < x_c$, i.e. no matter how complicated is the flow for $x < x_c$ it has no influence on the flow for $x > x_c$. However, there might be a problem of the type presented by Abramowicz & Kato (1989) in their Fig. 2: the flow passing through the critical point may formally reverse at some radius $x < x_c$, i.e. it may be globally impossible. This is not the case if the effective speed of sound is assumed to be constant also in the supersonic flow: our solutions continue smoothly all the way to the black hole.

We were not able to find steady-state solutions for $a > 0.14$. Perhaps physical solutions cannot pass a nodal point in the slow direction, and the accretion is non steady for $a > 0.14$. We shall explore the consequences of variable effective speed of sound in section 5.2.

4. Some Analytic Results

In order to have an analytic understanding of the behavior of the solutions and the dependence on the parameters a and v_s we attempt to replace eq. (14) by a simplified version of it, which retains the main topological features of the phase portrait, i.e. critical points and the 'Keplerian' curve, and also the dependence on a and v_s for small a 's. First let us define $\mu = v_s/a$ and $\nu_0 = v_0/a$, where v_0 , defined in eq.(18), is the 'Keplerian' radial velocity. Next we make the following assumptions

$$x' \approx 3; \quad \mu' \approx 1; \quad \nu_0' \approx 1; \quad (19)$$

which all follow from the assumption of $\alpha = 1$ and restricting the study to the vicinity of the Keplerian' curve (that includes the critical points). After these substitutions, being careful not to drop terms that are crucial for the main topological features, we end up with

$$\frac{d}{dx}, \quad p = \frac{(\alpha_0)}{6a_0(\alpha_0 - 1)}; \quad (20)$$

We see that the Keplerian' curve, for which $d = dx$ vanishes, and the critical points, where $\alpha_0 = 1$, are preserved.

Next, we try to find a workable approximation for $\alpha_0(x)$. To do so, we notice that the interesting transitions in the nature of the physical solution (Fig. 6) happens where the critical points are close to the maximum of $\alpha_0(x)$, which is also close to 1. With these approximations, we can use eq. (18) to get

$$\frac{d \ln \alpha_0}{dx}, \quad \frac{d \alpha_0}{dx}, \quad 1 = 3 - 2B(x - 3); \quad (21)$$

where

$$B^{-1} = 32 \frac{p}{6} a; \quad (22)$$

which can be integrated to give

$$\alpha_0(x) = 1 + B [(x_c - x_b)^2 - (x - x_b)^2]; \quad x_b = 3 + B^{-1} = 6; \quad (23)$$

x_c is the position of the critical point, which is related to b by setting $\alpha = 1$ in eq.(15), and x_b is the Saddle-Node bifurcation point, the boundary of the Saddle region and the Nodal region in Fig. 6.

Now, let us define the new variables ζ , and

$$B^{1/2} (x - x_b); \quad B^{1/2} \frac{p}{6a} = \left[\frac{6a}{32} \right]^{1/2}; \quad \alpha_0; \quad (24)$$

In terms of these new variables, eq.(20) becomes

$$\frac{d}{d\zeta} = \frac{1}{(1 + \zeta^2)(1 + \zeta^2)} + 2; \quad (25)$$

Now, it is easy to find the eigenmodes M of the critical point, by setting ζ equal to $M(\zeta_c)$ and requiring that it satisfies eq. (25) to the first order in ζ_c . This yields

$$M = \frac{1}{2} (1 - 4 \zeta_c + \frac{q}{1 - 8 \zeta_c}); \quad (26)$$

which already gives the three saddle, nodal and spiral regions in Fig. 6.

We do not intend to elaborate any further on the behavior of the solutions of eq.(25). This is mainly because the main property of the physical solution which is connecting the asymptotically Keplerian' curve to the critical point, is a global property and so its analytical investigation is not straightforward. The only clear conclusion that we can draw from eq.(25) is that the value of c for which the physical solution exists is a function of a . The transitions in the nature of the critical point, points B (SN) and C (NN) in Fig. 6, that were discussed in the last section, occur at specific values of c which can be already read from the numerical results in Fig. 6 and the definition of c in eq. (24)

$$s_N \approx 1.22; \quad n_N \approx 0.53; \quad (27)$$

Of course the advantage is that now we can apply this result to all small values of a and not only $a = 0.01$. This yields

$$\begin{aligned} \left(\frac{a}{0.01}\right) < \left(\frac{a}{0.14}\right)^3; & \quad \text{Nodal Point Through Slow Direction;} \\ \left(\frac{a}{0.14}\right)^3 < \left(\frac{a}{0.01}\right) < \left(\frac{a}{0.08}\right)^3; & \quad \text{Nodal Point Through Fast Direction;} \\ \left(\frac{a}{0.08}\right)^3 < \left(\frac{a}{0.01}\right); & \quad \text{Saddle Point;} \end{aligned} \quad (28)$$

The numerical values calculated for $a = 0.02$ agree very well with these scalings.

5. Discussion

After numerical and analytical study of the properties of the solutions of eq. (14) in the last two sections, we are now ready to discuss the physical picture within the framework of our approximations. Of course the question of accuracy of these approximations should be addressed as well, and we intend to do so, at least in part.

Our numerical solutions fully confirm our guesses that the angular momentum constant $l_0 = l_s$ (i.e. $b = 1$), and that $d \log l = d \log r = 2$ near r_s and for $r < r_m$ (cf. eq. 9, and the text between eq. 8 and 9). Note: we have not assumed that $l = l_s$, this was obtained numerically as a consequence of two conditions: the disk had to be nearly Keplerian at large radii, and the transition through the sonic point had to be smooth (cf eqs. 16).

5.1. Torque at the Sonic Point

The starting point of this investigation was a recent controversy about the sign of the torque at the sonic point of a thin accretion disk. The traditional picture of Novikov & Thorne (1973) argues for a zero torque boundary condition at the marginally stable orbit r_{ms} . Historically, the possibility of a significant torque at the sonic point due to strong magnetic fields was first brought up in Page & Thorne (1974). This issue was pursued more seriously by Krolík (1999), Gammie (1999), Agol & Krolík (2000).

It is easy to verify the validity of the traditional view in our model. Eq.(7) says that the magnitude of the torque is proportional to $(1 - \frac{1}{x})$ and eq.(9) gives $1 - \frac{1}{x}$ as a function of r and v . Let us find the ratio of $g(x_s)$ at the sonic point at $r_c = r_{ms}$, to $g(x)$ at, say $10r_{ms}$. Combining eqs. (4a), (6) and (7) we obtain

$$\frac{g(x_s)}{g(x)} = \frac{\frac{6a}{\frac{x^{1.5}}{2(x-1)}}}{1.5} = 2.8 \text{ at } x = 1; \quad \text{for } x = 30; \quad x = r = r_g; \quad (29)$$

Of course this result is valid only in the framework of our approximations, most crucially the assumption that the disk is thin and the accretion is steady. It is also not clear if the time averaged torque at r_{ms} would be affected by the fluctuations if the disk remained geometrically thin at r_{ms} at all time. We consider it likely that the time averaged inequality (29) would remain valid if the disk remained geometrically thin, while fluctuating in time.

Although some of the assumptions used in the derivation of eq. (29) may turn out to be incorrect, and the torque at the inner disk boundary may turn out to be large, we have not seen any convincing argument/paper that disproves the claim that the torque is very small if the disk is geometrically thin.

Note, that while our assumptions that the disk is geometrically thin and the accretion is steady state may be challenged, the same assumptions were adopted by Krolík (1999), Gammie (1999), and Agol & Krolík (2000), yet those authors came to a very different conclusion, and claimed that a torque at the inner disk edge may be large. We shall attempt to explain the reason for the difference in opinions in section (5.4).

5.2. Is constant v_s a good approximation?

Now is likely to have strictly constant effective speed of sound, and an important question is: does our model capture the essential properties of a thin accretion disk? A specific issue, brought up by Krolík (1999) is the possibility that the differential rotation

within the supersonic flow may increase the effective speed of sound so much that '... we expect the Alfvén speed in the uid frame to be c ...' (Krolik 1999). Obviously, if the magnetic field dominates the flow then the effective speed of sound is the same as Alfvén speed, and it also becomes relativistic.

The largest energetically possible increase of the effective speed of sound may be obtained by assuming a quasi-adiabatic flow: all energy transferred from differential rotation into the accretion flow is used to increase magnetic energy, and none is radiated away. This is certainly a limit which is not likely to be reached in realistic flows. Nevertheless, we explored this possibility as a limiting case, and we refer to it as a quasi-adiabatic approximation.

We repeated the calculations of our models with $a = 0.01$: in the first model we adopted $\alpha = 0.01$, and in the second $\alpha = 0.1$, and we obtained: $x_c = 2.82859$, $b = 1.00068$ for the first model, and $x_c = 3.04505$, $b = 0.99636$, for the second. Obviously, these values were identical to the models described in section 3. We continued these solutions some distance into the supersonic part of the flow, down to a transition radius x_{tr} , where we abruptly switched the flow from having constant effective speed of sound $v_s = 0.01c$, and constant α , to a quasi-adiabatic approximation. In this approximation the energy of differential rotation was fully used to increase the energy of tangled magnetic fields. We assumed that at x_{tr} the ratio of magnetic pressure to total pressure was equal to β . For $r < r_{tr}$ the energy of differential rotation was pumped into the magnetic field, hence the magnetic pressure increased, while the gas pressure was assumed to change adiabatically, i.e. the gas pressure decreased because of decompression. Therefore, the ratio P_{mag}/P_{tot} increased down the flow for $x < x_{tr}$, and the parameter β increased correspondingly. We assumed that hydrostatic equilibrium was maintained in the direction perpendicular to the disk equatorial plane, as that is established on a fraction of rotational period, while the flow followed many rotations prior to crossing the black hole horizon. The gas density rapidly decreased as the flow accelerated toward the black hole and expanded in vertical direction. The vertical expansion of the flow was a consequence of the increase in the effective speed of sound, which became practically equal to the Alfvén speed.

We found that if the transition from a flow with $v_s = ac = \text{const}$ to a quasi-adiabatic flow was made sufficiently far into the supersonic region, with $x_{tr} < 2.79$ and $x_{tr} < 2.78$ for the two models, respectively, the flow proceeded smoothly all the way to the black hole, and remained similar to the flow in our original model. At the transition radius, $x_{tr} = 2.8$, the flow was moderately supersonic, with the effective Mach number of 1.3 and 2.4, for the two cases, respectively. Down the flow, for $x < x_{tr}$, the magnetic pressure increased, and the parameter β also increased to 1. The effective speed of sound gradually increased by

a factor 3, thereby increasing the flow thickness correspondingly, but the flow remained supersonic.

When the transition was made at a larger value of x_{tr} , i.e. at a smaller effective Mach number, the flow pattern was initially normal, i.e. the , the effective Mach number and the Alfvén speed all increased gradually with decreasing radius. However, at still smaller radii the flow became sub-sonic and the numerical solution 'reversed' toward large radii, a possibility pointed out by Abramowicz & Kato (1989). Superficially a global steady state solution did not exist for the transition radius larger than approximately $2.8r_g$. However, it is virtually certain that as the flow tried to 'reverse', a shock wave would form. It is not clear that a steady state flow could not be maintained, with the second sonic point located down the flow from the shock location, and the matter ultimately plunging into the black hole. However, these complexities are beyond the scope of our paper.

The results of our numerical experiment are easy to understand: as the dissipation of magnetic energy is switched on (quasi-adiabatic approximation) the magnetic pressure builds up, and the flow expands in vertical direction. Had the transition been made at a large radius, the disk would become geometrically thick. The very assumption that the disk is thin is obviously equivalent to the assumption that the dissipation of magnetic field is efficient. Note, there is no fundamental difference between the sub-sonic and supersonic flow, with the gas moving along a spiral which gradually becomes less tight as the radius decreases. Inwards of the critical point the flow makes a large number of rotations, which are responsible for the buildup of the magnetic field in the quasi-adiabatic approximation. It is natural to expect that the time scale for dissipation is comparable to the time scale of the buildup, as otherwise geometrically thin disk could not exist.

Note: the shear $jd = dr/j$ increases inwards gradually, and it experiences no dramatic change at $x_c = 3$. As long as radial velocity remains much smaller than rotational velocity there is no dramatic difference in physical processes between the subsonic flow at $x > x_c$, and supersonic flow at $x < x_c$. A true 'plunging' region is at $x < 2$, where the radial velocity becomes comparable to the rotational velocity.

While we cannot prove or disprove the sensibility of a quasi-adiabatic approximation, we think that a constant effective speed of sound is physically more plausible. It is more or less equivalent to the assumption that a relation between the buildup and the dissipation of magnetic fields is similar in the supersonic and in the sub-sonic disk accretion flow.

5.3. Is Nodal Passage in the Slow Direction Physical?

Inspection of Figs. 2, 3, 4, 7, 8, 9, and 10 shows that the geometry of transonic flow appears to be similar when the critical point is of a saddle type or a nodal type, provided the solution passes the latter in the fast direction. The transition from the saddle to the nodal (fast) geometry is smooth, with no apparent problem. The sub-sonic flow connects well to a Keplerian disk at large radii, and the supersonic flow approaches a free fall at small radii. This trouble free region corresponds to the aBC segment (thick line) in Fig. 6, which ends at point C, where it contacts the borderline of the red points of the spiral type, and where $\alpha = 0.14$. Obviously, no physical solution can pass through a spiral point. Above point C the analytical solutions pass the nodal critical point in the slow direction, and these solutions do not appear to be physical (cf. Fig. 11), as there is a sharp change in the slope of the solution (see the end of Sec. 3). We do not know if they are unstable, or perhaps no truly steady-state flow is possible for $\alpha > 0.14$ (for $\alpha = 0.01$).

The study of the stability of these points with the assumption of constant v_s and α is even less satisfactory than the steady state solutions. Nevertheless, Kato, Honma, and Matsumoto (1988) show that, within these assumptions, local instabilities occur when

$$ss(r_c) > \frac{dv}{dr} \Big|_{\text{dot}}; \quad (30)$$

where ss is the Shakura-Sunyaev value of α ($ss = 2.1$). The dotted portion of the physical curve in Fig. 7, which covers almost all of the sector Cd, shows the critical points that satisfy this criterion. This indicates that the nodal passage in the slow direction is probably unstable. We should point out that, contrary to the conventional picture (originally suggested by Matsumoto et al. 1984), this is not a generic property of the nodal critical points, but a generic property of the passage in the slow direction of the nodal point, where $|dv/dr|$ in eq. (30) is small.

We cannot prove that the transition through a nodal-type point in the fast direction is the only physically acceptable solution, i.e. that it is unique, but this seems to be likely upon inspection of Figs. 9, 10, 11, 12, and it also agrees with the finding of Abramova et al. (2001). If correct, this could resolve the ambiguity discovered by Matsumoto et al. (1984). Unfortunately, we cannot offer a simple physical explanation for the transition from saddle-type to nodal-type critical points while the parameter α increases. We stress that the physical nature of nodal points is outside the scope of our paper, which is concentrated on the issue of the inner boundary condition for geometrically thin steady state accretion disks.

5.4. Discussion of Gammie (1999) paper

There remains the issue which gave rise to this paper: why did Krolik (1999), Gammie (1999) and Agol & Krolik (2000) claim that the no torque inner boundary condition is incorrect even for thin, steady state disks? Let us consider the case presented by Gammie (1999), as he provides the fullest model calculation. Gammie assumed that '... the disk is thin, $c_s^2 = c^2 = 1$...', and '... that $c_s^2 = 1$ so that magnetic fields make a negligible contribution to the hydrostatic equilibrium of the disk ...'. He also writes: 'This picture leads one to consider a steady, axisymmetric flow close to the equatorial plane of the Kerr metric.' These assumptions are practically identical to ours.

Some of the assumptions we made in this paper, and some made by Gammie are the same: we all assume that geometrically thin steady state accretion disks exist, and that within a thin disk magnetic field is relatively weak. Therefore c_s^2 is small, say $c_s^2 = 0.1$, or so. Hence, the effective speed of sound in the disk is practically equal to the gas speed of sound. Our model with a constant and small effective speed of sound implies that the flow remains geometrically thin also in the supersonic region, for $r < r_{ms}$. Gammie also assume that the flow is geometrically thin there, in fact his flow thickness for $r < r_{ms}$ is decreasing in proportion to the radius r (cf. his eq. 4).

A disagreement appears in the treatment of the transition from the flow at $r > r_{in} = r_{ms}$, to the flow at $r < r_{in}$. We require the transition from sub-sonic to supersonic flow to pass smoothly through a critical (sonic) point. Gammie has no smooth transition at his r_{in} . Rather at r_{in} his model undergoes a dramatic jump in the assumed physical conditions. The flow is gas dominated and has a negligible magnetic field for $r > r_{in}$, and it has no gas pressure and is magnetic field dominated for $r < r_{in}$. No justification is offered for this jump at r_{in} .

Gammie (1999) makes additional assumptions about the flow for $r < r_{in}$:

- The magneto-rotational instability does not operate.
- There is no dissipation of the magnetic field.
- The thickness of the flow is proportional to radius.

No justification is offered for these assumptions. As far as we can tell all these assumptions are incorrect. The magneto-rotational instability makes magnetic fields tangled in a single rotation period, while the assumption (a) is needed to maintain a well ordered magnetic field. Once the fields are tangled the dissipation is unavoidable (e.g. Igumenshchev & Narayan 2002). The magnetic field increases in strength as a result of strong differential rotation, the effective speed of sound increases rapidly, and the flow must expand in vertical

direction because dynamical time scale is equal to a fraction of the rotation period, while the flow along a spiral makes many rotations for $r < r_{in}$. In fact without many rotations a large increase in the magnetic field strength would be impossible. Hence, the assumptions (a) and (b) are incompatible with each other: as the magnetic pressure and the Alfvén speed increase strongly with decreasing radius, the flow cannot contract in the z' direction. If the expansion in the z' direction were allowed for, the strength of the magnetic field and the magnetic torque would be reduced.

However, the main conceptual problem with the model is that the two parts of the flow: the disk for $r > r_{in}$ and the 'plunging region' for $r < r_{in}$, are not connected physically, as they are governed by incompatible approximations, with no smooth transition between them. For these reasons we think that Gammie's model is not relevant to the issue: is the no torque inner boundary condition correct or not.

A large part of Agol & Krolik (2000) analysis remains correct: there may be a torque applied to the inner edge of the accretion disk provided there is a large scale magnetic field, possibly threading the black hole. This is a modified Blandford-Znajek mechanism (e.g. Li 2000, Wang et al. 2002, and references therein). The gaseous disk may remain geometrically thin while the stresses are transmitted by a large scale magnetic field which has a vertical scale height comparable to radius. This is a picture which is conceptually very different from the case considered by us and by Gammie (1999), as we and Gammie assume that the magnetic fields are connected to a geometrically thin flow.

6. Conclusions

The condition given with the eq. (1) of this paper is local, and it is valid even if the parameter varies with radius. It requires the assumption of a steady state to hold. However, we think it is reasonable to expect that it also holds for a disk with an accretion which is steady in a statistical sense only, as long as the disk thickness does not exceed the value $H \ll r$ throughout the fluctuations cycle. There is a simple physical reason for this assertion: as long as the disk remains geometrically thin the total pressure within it remains low and hence the stresses responsible for transferring angular momentum remain low. Obviously, it is important to verify this claim with the full 3-D time dependent simulations. However, current numerical models are limited by the available computer power to disks which are much thicker than the one considered in this paper and also by the absence of cooling processes which are essential for the formation of thin disks. At this time there is no observational or theoretical reason to exclude the possibility that geometrically thin disks exist. Currently, there is also no way to prove they exist, as the relevant thickness

is that of the layer over which the magnetic fields transferring angular momentum extend, and this quantity is not readily observable.

We have found a unique steady state solution for a simple model with a constant effective speed of sound $v_s = 0.01c$, and a given viscosity parameter $\kappa < 0.14$. The solution was found by approaching the critical point from large radii, i.e. from the sub-sonic flow side. The supersonic flow had no effect on the critical point, as expected on general grounds. In particular, we demonstrated that, for geometrically thin flow, there is no global problem of the type envisioned by Abramowicz & Kato (1989) in their Fig. 2. Once the flow passes the critical point it plunges into the black hole along a spiral, roughly conserving angular momentum, as asserted in many papers written in the 1980s.

In our disk model the torque at the sonic point is very small (cf. eq. 1 and 29), and hence the so called 'zero torque' inner boundary condition is a good approximation for our geometrically thin steady state disk. We emphasize that the disk thickness H must include the thickness of magnetic structures responsible for angular momentum transfer, not just the thickness of the gas layer. The effective speed of sound v_s is affected by the total pressure, which includes the contribution of magnetic pressure (cf. eq. 5b).

Just as discovered by Matsumoto et al. (1984) we also found that the critical point is of the saddle-type for small values of κ , and becomes a nodal-type for large κ , in our case for $\kappa > 0.08$. Unfortunately, we cannot provide a simple physical explanation for this transition. However, we presented plausible arguments that the transition through the nodal-type critical point is unique, as there is only one solution which appears to be smooth. This was also demonstrated by Artemova et al. (2001).

We found that our steady state solutions exist only for $\kappa < 0.14$ ($100v_s=c$)^{1/3}, and it appears that there are no physically sensible solutions for $\kappa > \kappa_{\text{crit}} = 0.14$ ($100v_s=c$)^{1/3}. It is not clear if this is a general result or just an artifact due to simplicity of our model. The issue is not the particular value of κ_{crit} , which is certainly model dependent, but the very existence of κ_{crit} . Unfortunately, we cannot offer a simple physical explanation for this finding.

Note: a thin disk may be subject to a significant torque at its inner edge if there is a large scale magnetic field, like that proposed for the modified Blandford-Znajek mechanism, also referred to as a magnetic coupling model (e.g. Agol & Krolik 2000, Li 2000, Wang et al. 2002, and references therein).

Our assumption that the accretion flow remains geometrically thin at all radii: in the sub-sonic part for $r > r_{\text{cr}}$, and in the supersonic part for $r < r_{\text{cr}}$, is physically equivalent to the assumption that magnetic fields dissipate effectively at all radii. If the dissipation

becomes inefficient at some transition radius r_{tr} , than the magnetic field pressure and the disk thickness increase rapidly for $r < r_{tr}$. This transition affects the flow very little if $r_{tr} < 2.8r_g$: the infall towards the black hole proceeds along a tight spiral and it remains supersonic. However, if $r_{tr} > 2.8r_g$ the increase of the magnetic pressure and the disk thickness is so strong, that the accretion flow is drastically affected. We provide a very brief description of such a flow in section 5.2. However, the opponents of the 'no torque inner boundary condition' have not investigated this possibility at all. In particular Gammie (1999) assumed that the flow remains geometrically thin at all radii, yet he claimed that there is a large torque at $r = r_{in}$. This assertion is based on a model calculated with inconsistent assumptions, and a huge jump in physical conditions at $r_{in} = r_{in}$ (cf. section 5.4 of this paper). Therefore, this paper does not provide a credible case against the 'no torque inner boundary condition' in thin accretion flows.

We are very grateful to the anonymous referee who relentlessly pressured us to refine our analysis. It is a great pleasure to acknowledge many useful and critical comments by Dr. J. Goodman.

REFERENCES

Abramowicz, M. A., Jaroszynski, M. & Kozlowski, M. 1978, *A & A*, 63, 209
 Abramowicz, M. A., & Kato, S. 1989, *ApJ*, 336, 304
 Agol, E., & Krolík, J. H. 2000, *ApJ*, 528, 161
 Agol, E., Krolík, J., Turner, N. J. & Stone, J. M. 2001, *ApJ*, 558, 543
 Abramitative, P. J. 1998, *ApJ*, 501, L189
 Abramitative, P. J. 2001, *astro-ph/0110250*
 Abramitative, P. J. 2001, *astro-ph/0110670*
 Abramitative, P. J. & Narayan, P. 1999, *ApJ*, 523, L7
 Abramitative, P. J., Reynolds, C. S. & Chiang, J. 2001, *ApJ*, 548, 868
 Artemova, I. V. et al. 2001, *ApJ*, 549, 1050
 Balbus, A. S. & Hawley, J. F. 1991, *ApJ*, 376, 214
 Balbus, A. S. & Hawley, J. F. 1991, *ApJ*, 376, 214
 Ball, G. H., Narayan, R. & Quataert, E. 2001, *ApJ*, 552, 221
 Blaes, O. et al. 2001, *astro-ph/0108451*
 Blandford, R. D. & Znajek, R. L. 1977, *MNRAS*, 179, 433

Cunningham, C. T. 1975, *ApJ*, 202, 788

Cunningham, C. T. 1976, *ApJ*, 208, 534

Flemming, T. P., Stone, J. M. & Hawley, J. F. 2000, *ApJ*, 530, 464

Galeev, A. A., Rosner, R. & Vaiana, G. S. 1979, *ApJ*, 229, 318

Gammie, C. F. 1999, *ApJ*, 522, L57

Guckenheimer, J., Holmes, P., 'Nonlinear Oscillations, Dynamical Systems, and Bifurcation of Vector Fields', 1983, Springer

Hawley, J. F. & Balbus, A. S. 1991, *ApJ*, 376, 223

Hawley, J. F. & Krolík, J. H. 2002, *ApJ*, 566, 164

Hawley, J. F., Balbus, S. A., & Stone, J. M. 2001, *ApJ*, 554, L49

Igumenshchev, I. V. & Narayan, R. 2002, *ApJ*, 566, 137

Krolík, J. H. 1999, *ApJ*, 515, L73

Krolík, J. H. & Hawley, J. F. 2002, *ApJ*, 573, 754

Li, L.-X. 2000a, *ApJ*, 531, L111

Li, L.-X. 2000b, *ApJ*, 533, L115

Lin, D. N. C. & Papaloizou, J. C. B. 1996, *ARA&A*, 34, 205

Lynden-Bell, D. & Pringle, J. E. 1974, *MNRAS*, 168, 603

Matsumoto, R. et al. 1984, *PASJ*, 36, 71

Muchotrzeb, B. & Paczynski, B. 1982, *A&A*, 32, 1

Novikov, I. D. & Thorne, K. S. 1973, In 'Black Holes - Les Astres Occlus', Eds: C. De Witt & B. S. De Witt, New York: Gordon & Breach

Paczynski, B. 2000, [astro-ph/0004129](#)

Paczynski, B. & Wijita, P. 1980, *A&A*, 88, 23

Page, D. N., & Thorne, K. S. 1974, *ApJ*, 191, 1974

Parker, E. N. 1958, *ApJ*, 128, 664

Pringle, J. E. 1981, *ARA&A*, 19, 137

Pringle, J. E. & Rees, M. J. 1972, *A&A*, 21, 1

Reynolds, C. S. & Armitage, P. J. 2001, *ApJ*, 561, L81

Reynolds, C. S., Armitage, P. J. & Chiang, J. 2001, 20th Texas Symposium, AIP Conf. Proc. Vol. 586, p. 668 (Eds.: J. C. Wheeler, & H. Martel) = [astro-ph/0102045](#)

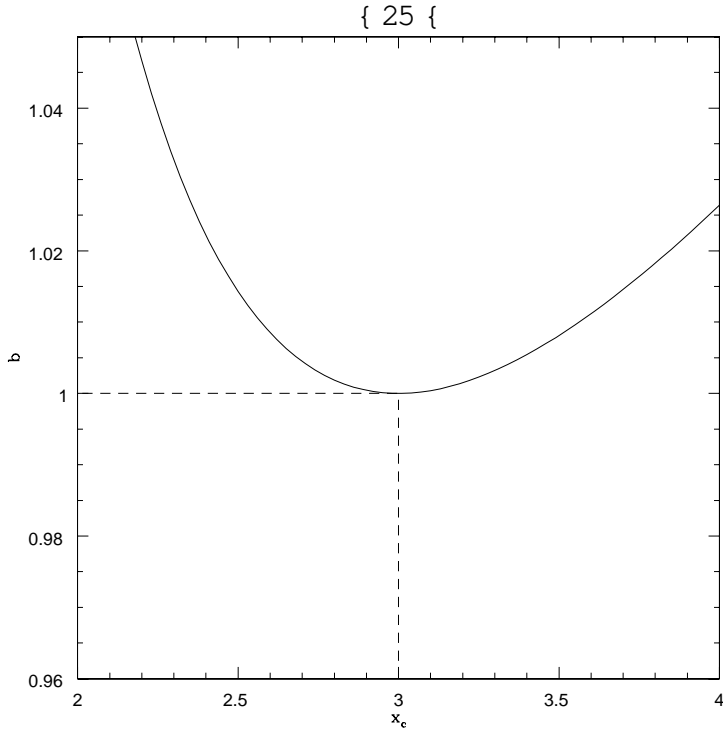


Fig. 1. The angular momentum constant b is shown as a function of the position of the critical point x_c for $a \neq 0$. We see that, for $b > 1$, there are two fixed points, at $b = 1$, there is one degenerate fixed point at $x = 3$ (marginally stable orbit), and for $b < 1$ no fixed point exist.

Sano, T. & Inutsuka, S.-I. 2001, ApJ, 561, L179

Shakura, N. I. & Sunyayev, R. A. 1973, A & A, 24, 337

Stoeger, W. R. 1976, A & A, 53, 267

Stone, S. & Pringle, J. E. 2001, MNRAS, 322, 461

Stone, J. M., Pringle, J. E. & Begelman, M. C. 1999, MNRAS, 310, 1002

Wang, D. X., Xiao, K., & Lei, W. H. 2002, astro-ph/0209368

Wijmans, J. et al. 2001, MNRAS, 328, L27

{ 26 }

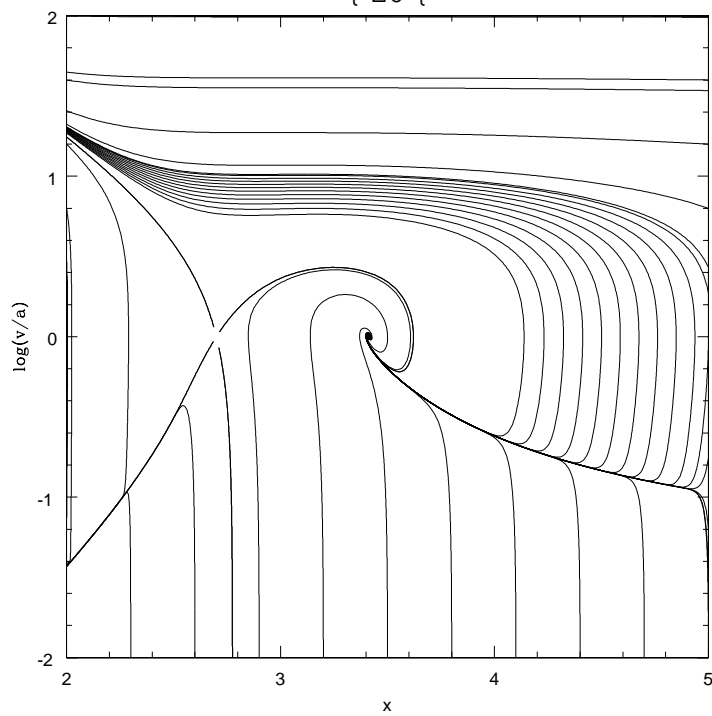


Fig. 2.1 The Phase Portrait for $a = 0.01$; $= 0.15$ and $b = 0.9997$. There is a saddle point at $x = 2.7$ and a spiral point at $x = 3.4$.

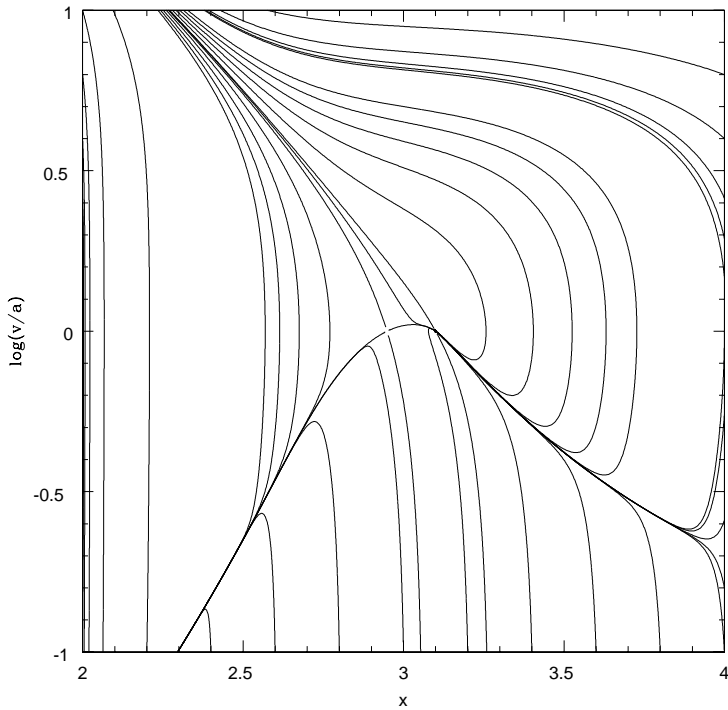


Fig. 3.1 The Phase Portrait for $a = 0.01$; $= 0.15$ and $b = 0.9949$. There is a saddle point at $x = 2.94$ and a nodal point at $x = 3.1$.

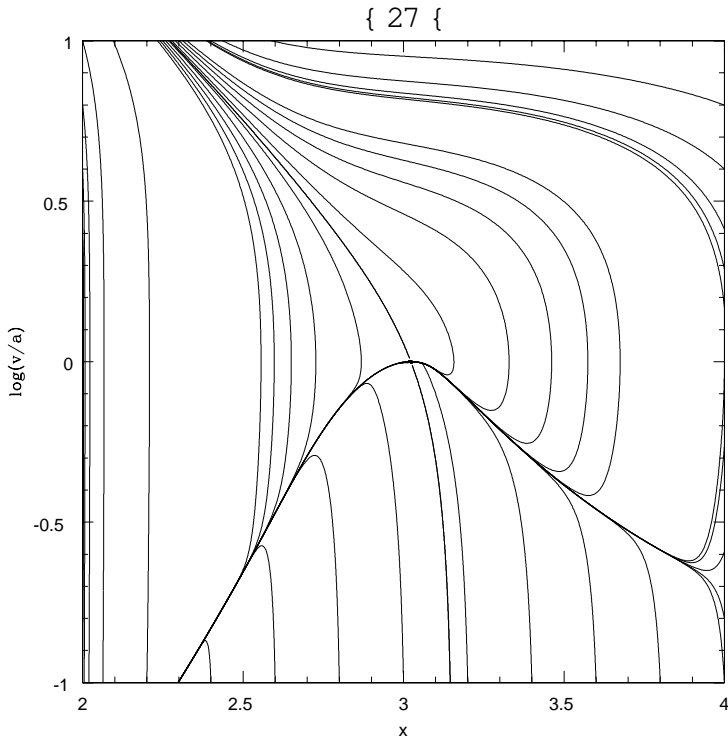


Fig. 4. The Phase Portrait for $a = 0.01$; $= 0.15$ and $b = 0.9947$. There is a degenerate saddle-node point at $x = 3.0228$.

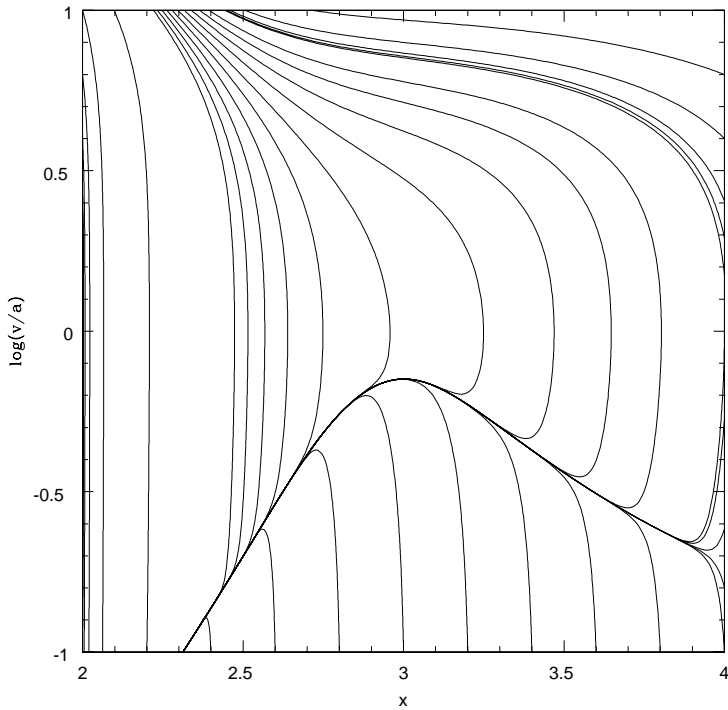


Fig. 5. The Phase Portrait for $a = 0.01$; $= 0.15$ and $b = 0.9927$. There is no fixed point for these parameters.

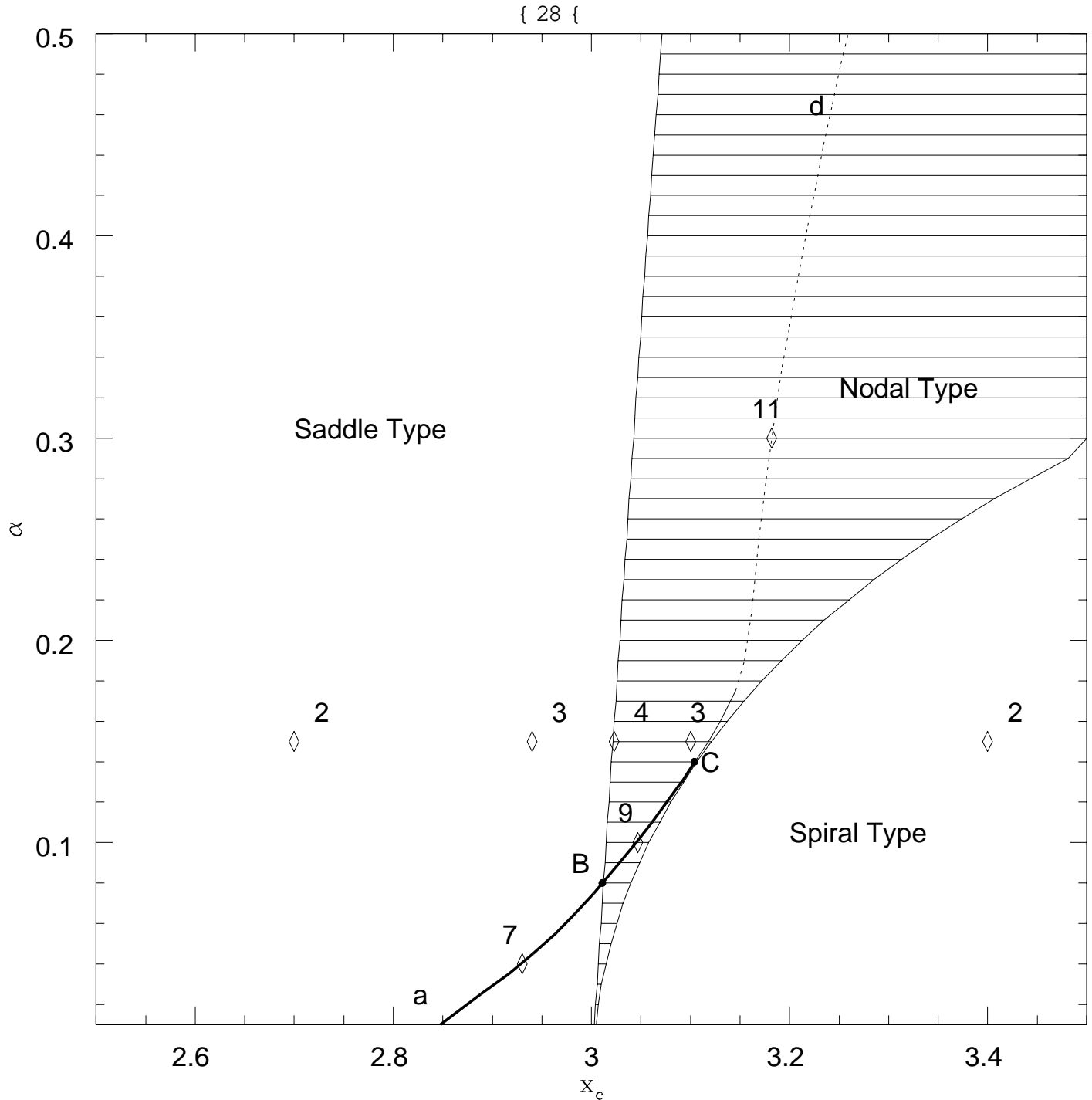


Fig. 6. The parameter space of the problem for $a = v_s = c = 0.01$. x_c is the radius of the critical point in units of r_g and α is the viscosity parameter. The curve $aBcd$ shows the position of the fixed points that allow physical solutions (cf. Sec. 3), while the dotted section of the curve are unstable solutions according to eq. (30). Also the parameters of phase portraits in the other figures are represented by numbered diamonds. The number of each diamond is the number of the associated figure in this paper. The Phase Portrait presented in Fig. 5 has no fixed points, and therefore it is not represented in this figure.

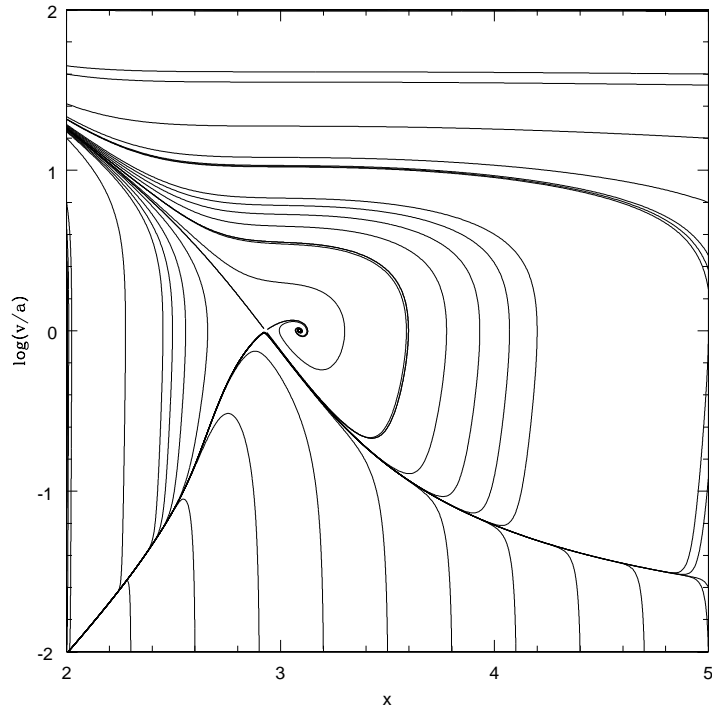


Fig. 7.1 The Phase Portrait for $a = 0.01$; $= 0.04$ and $x_c = 2.930$. The physical solution (thick curve) passes a critical point of the saddle type.

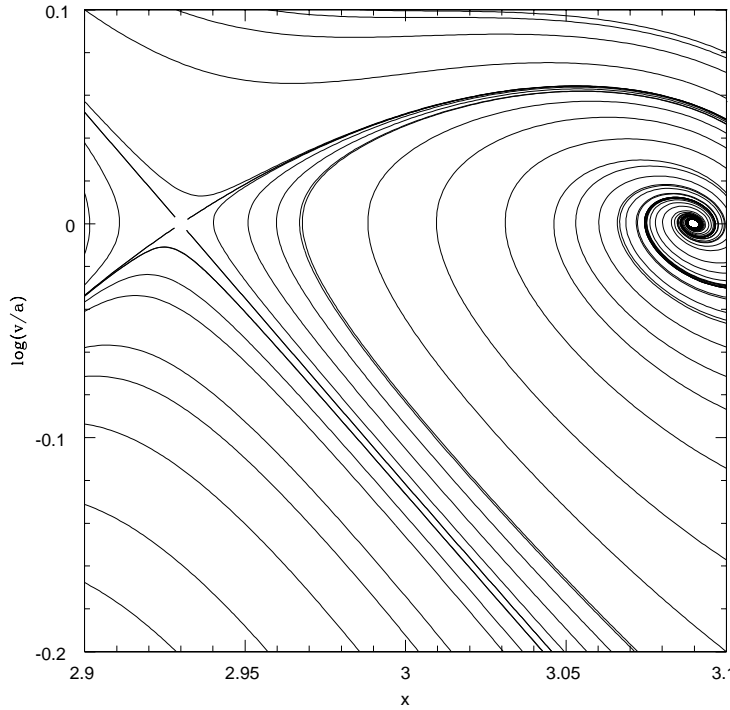


Fig. 8.1 The vicinity of the critical points in the phase portrait of Fig. 7.

{ 30 }

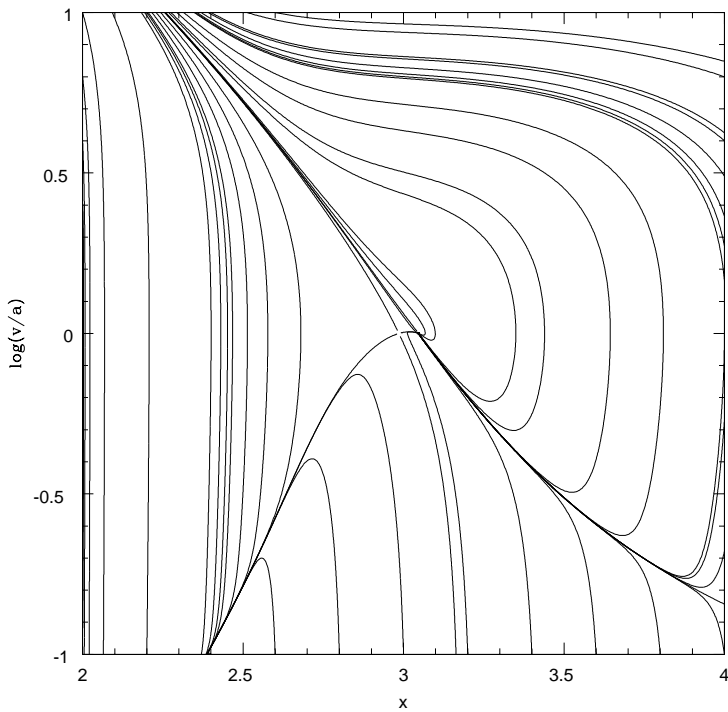


Fig. 9. The Phase Portrait for $a = 0.01$; $= 0.1$ and $x_c = 3.047$. The physical solution (thick curve) passes a critical point of the nodal type, in the fast direction.

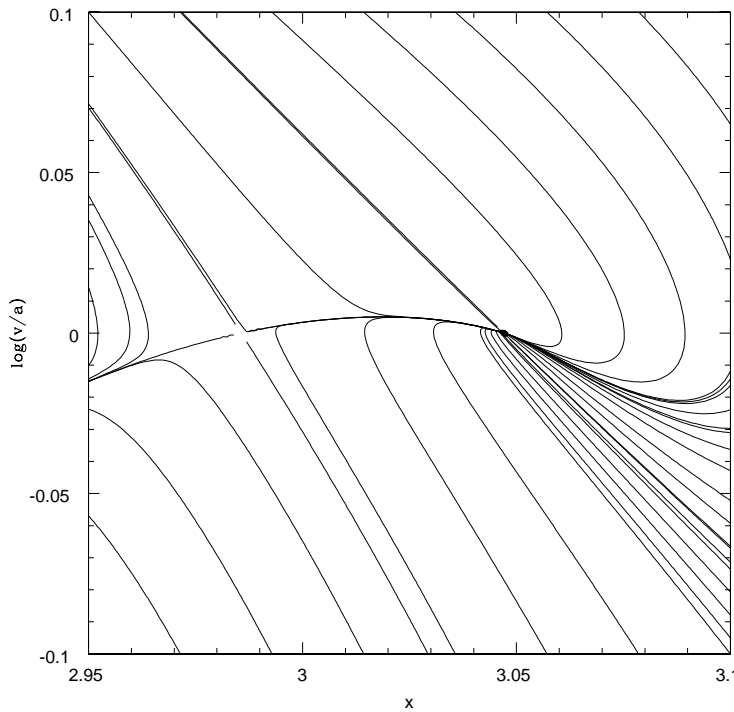


Fig. 10. The vicinity of the critical points in the phase portrait of Fig. (9).

{ 31 }

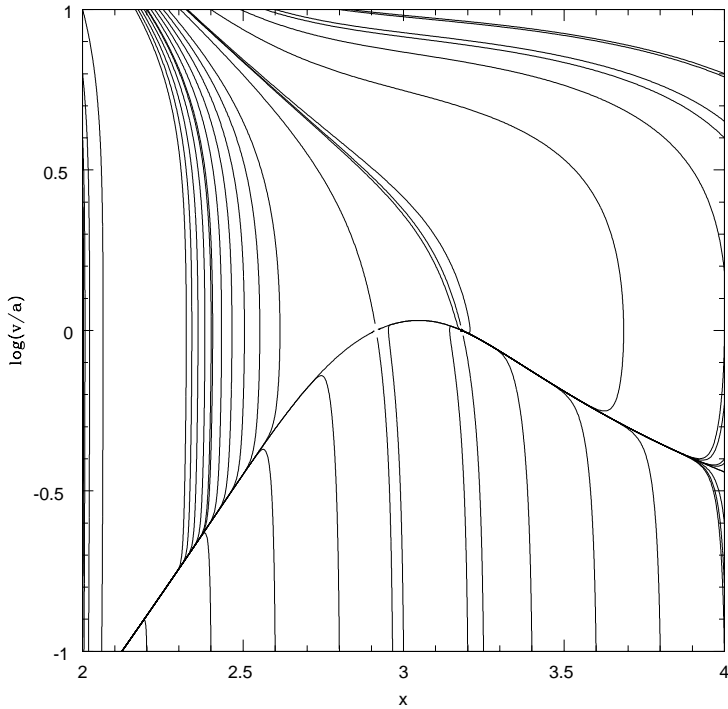


Fig. 11. The Phase Portrait for $a = 0.01$; $= 0.3$ and $x_c = 3.183$. The physical solution (thick curve) passes a critical point of the nodal type, in the slow direction, analytically.

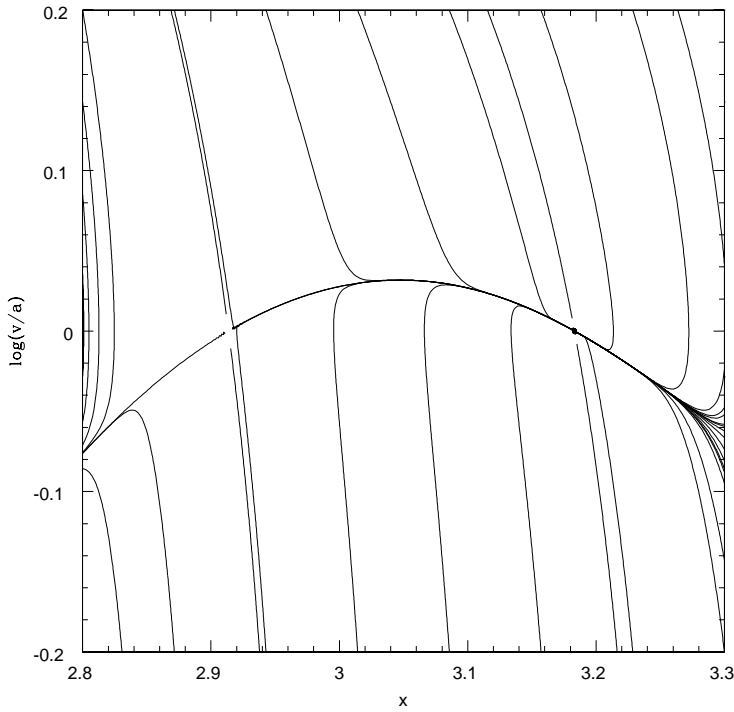


Fig. 12. The vicinity of the critical points in the phase portrait of Fig. (11).